"BOUNDARY VOLTAGE LIMITS" – AN INSTRUMENT TO INCREASE THE UTILIZATION OF THE EXISTING INFRASTRUCTURES

Daniel-Leon Schultis*, Albana Ilo

TU Wien – Institute of Energy Systems and Electrical Drives, Vienna, Austria
**daniel-leon.schultis@tuwien.ac.at*

Keywords: *LINK*-BASED HOLISTIC ARCHITECTURE, LOW VOLTAGE GRIDS, USE CASE, LUMPED MODELLING, BOUNDARY VOLTAGE LIMITS

Abstract

The compliance to the voltage limits defined by grid codes is the major hurdle for the large scale integration of distributed energy resources. The conventional approach, in which the state of the medium voltage grid is calculated and checked against constant limits, does not support the complete utilization of the existing infrastructures: narrow voltage limits are set in medium voltage level that guarantee limit compliance in low voltage level also under worst case conditions. This paper uses the *LINK*-based holistic architecture to extend the lumped model of low voltage grids by variable boundary voltage limits (BVL).This ensures internal limit compliance without involving safety margins when calculating and operating medium voltage grid. The BVLs are quantified for different test grids and the effect of the feeder properties on the limit deformation is identified. The formulated use case allows to operate medium voltage grids closer to their factual limits, increasing the utilization degree of infrastructures.

1 Introduction

The power system is often referred to as the biggest and most complex man-made system existing on earth. Its complete modelling is impracticable due to the related modelling effort, the required computational resources and unknown system details. Therefore, power system analysis is restricted to relative small grid parts, where lumped models represent the neighboured grid parts. The compilation of the latter is a challenging task as these parts usually include numerous elements with distinct characteristics and complex interdependencies.

One of the base quality parameters of power systems is the voltage. The grid code stipulates European distribution system operators (DSO) to maintain the voltages at the connection nodes of customer plants (CP) between ±10% around the nominal value [1]. The compliance to these limits is traditionally addressed on the planning level by respecting predefined voltage bands in different voltage levels. The on-load tap changer of the supplying transformer keeps the voltage at its secondary bus within a predefined band. From thereon, the remaining voltage band is allocated between the medium (MV) and low voltage (LV) level [2], and the grids are dimensioned accordingly. Nowadays, the development towards Smart Grids involves an improved monitoring and controlling of distribution systems, enabling the online verification of voltage limit compliance. For this purpose, the voltages in MV level are calculated and checked against constant voltage limits. LV grids are represented by lumped models that represent their $P_t(U_t)$ and $Q_t(U_t)$ behaviour. The conventional approach to guarantee limit compliance of the voltage at the LV-CP boundary nodes is to set tighter limits for the MV level to imply safety margins for the voltages in LV level. These safety margins reduce the hosting capacity of LV grids and consequently hinder the optimal utilisation of the existing electricity infrastructure.

This paper improves the conventional lumped model of LV grids to consider their factual voltage profiles. It extends the model by so-called "boundary voltage limits" (BVL) that allow to operate MV grids closer to their factual limits. Section 2 describes the methodology underlying the model extension. The modelling according to the *LINK*-based holistic architecture is shown in section 3. This is followed by a discussion of the variable boundary voltage limits in section 4. Section 5 introduces a use case that allows to utilize them for smart grid operation. Conclusions are drawn in section 6.

2. Methodology

This work applies the *LINK*-based holistic architecture [3] and qualitative research methods to expand the lumped model of LV grids by a new parameter, i.e. the "Variable Boundary Voltage Limits", and to derive use cases for smart grid operation. Numerical analysis is used to quantify the introduced parameters for different LV grids.

3. Modelling based on *LINK*-architecture

The *LINK*-based holistic architecture provides a systematic approach for power system modelling as it relies on the

fractal feature of power systems [4]. It divides the entire electricity grid into well-defined Grid-, Producer- and Storage-Links that fit into one another to establish flexible chains over the vertical and horizontal power system axes. Each Link is composed of electrical appliances, the corresponding controlling schema, and the interface(s). The Grid-Links include Volt/var secondary controls (Vv**SC**) that calculate set points for the available control variables while respecting constraints at the boundaries to neighbour Grid-Links, Fig. 1. The entirety of all lines and cables, transformers and reactive power devices included in a Grid-Link is denoted as "Link-Grid".

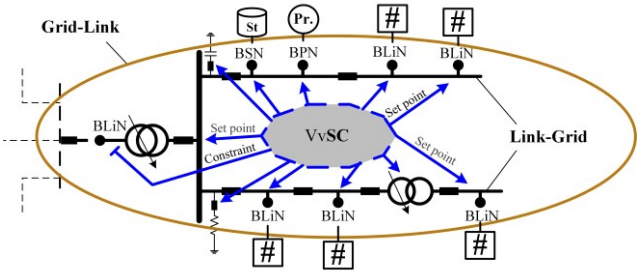

Fig. 1 Overview of the Grid-Link.

The lumped models of neighbour Link-Grids, Producers and Storages are represented by the #, Pr, and St symbols, respectively, and are connected to the MV_Link-Grid through Boundary Link Nodes (BLiN), Boundary Producer Nodes (BPN), and Boundary Storage Nodes (BSN).

3.1 Lumped modelling of low voltage grids

To conduct load flow analysis in MV level, the MV grid itself is modelled in detail, while lumped models represent the connected LV grids.

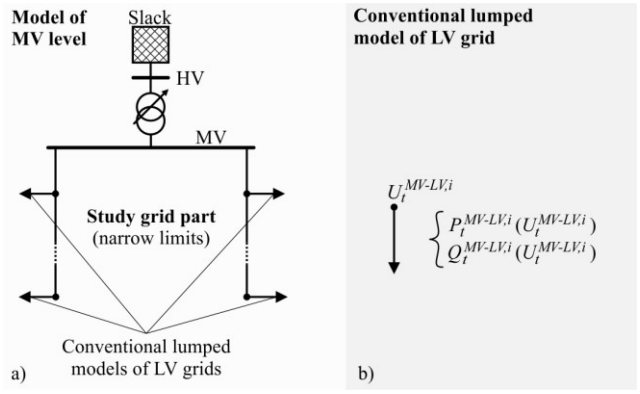

Fig. 2 Setting used to perform the conventional load flow analysis in MV level: (a) model of MV level; (b) lumped model of LV grids.

3.1.1 Conventional approach

Fig. 2 shows an overview of the conventional load flow analysis in MV level. The LV grids are modelled as PQ node-elements, which are commonly represented by the "→" symbol in load flow analysis tools, Fig. 2a. In the general case, the active ($P_t^{MV\text{-}LV,i}$) and reactive power ($Q_t^{MV\text{-}LV,i}$) contributions of each LV grid (with index i) are defined for each instant of time (t) as functions of the voltage ($U_t^{MV\text{-}LV,i}$) at its terminal, Fig. 2b. No voltage limits are associated to these elements. Instead, limit compliance in LV level is verified by checking the voltages of all MV nodes against narrow limits, e.g. from 0.95 to 1.05 p.u. In this case, the same voltage limits are set for each MV node and each instant of time, Fig. 3.

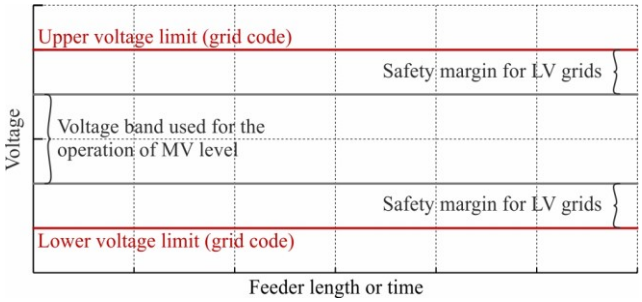

Fig. 3 Traditional voltage bands for the MV and LV level.

3.1.2 LINK-based approach

Fig. 4 shows an overview of the setting used to perform the *LINK*-based load flow analysis in MV level.

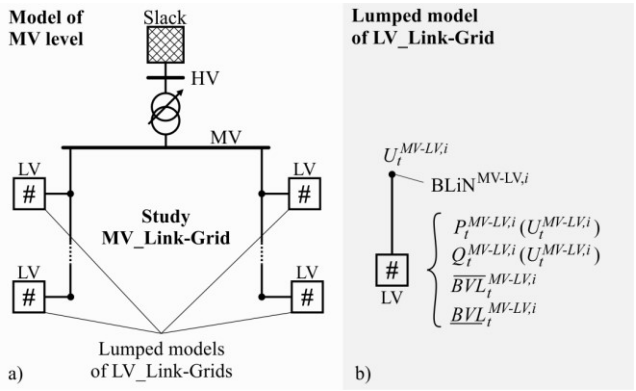

Fig. 4 Setting used to perform the *LINK*-based load flow analysis in MV level: (a) model of MV level; (b) lumped model of LV_Link-Grids.

In addition to the $P_t(U_t)$ and $Q_t(U_t)$ curves of the conventional lumped LV grid models, they include upper $\overline{BVL}_t^{MV\text{-}LV,i}$ and lower boundary voltage limits $\underline{BVL}_t^{MV\text{-}LV,i}$ that vary over time. These boundary voltage limits pertain to the corresponding MV-LV boundary link node ($BLiN^{MV\text{-}LV,i}$); their compliance guarantees that no limit violations occur within the represented LV_Link-Grid. In this case, individual limits are used for each $BLiN^{MV\text{-}LV,i}$ and each instant of time.

3.2 Model description

The detailed LV_Link-Grid model and the lumped models of the connected CP_Link-Grids are needed to calculate the BVLs of the lumped LV_Link-Grid model.

3.2.1 Customer plant

The lumped model of the residential CPs (with index *j*) includes one equivalent device and one producer model, which represent the household appliances and the photovoltaic (PV) system, respectively, Fig. 5a. The grid code requirements are reflected by time-constant upper ($\overline{BVL}_t^{LV\text{-}CP_j}$) and lower BVLs ($\underline{BVL}_t^{LV\text{-}CP_j}$) pertaining at the LV-CP boundary nodes (BLiN$^{\text{LV-CP}_j}$), Fig 5b.

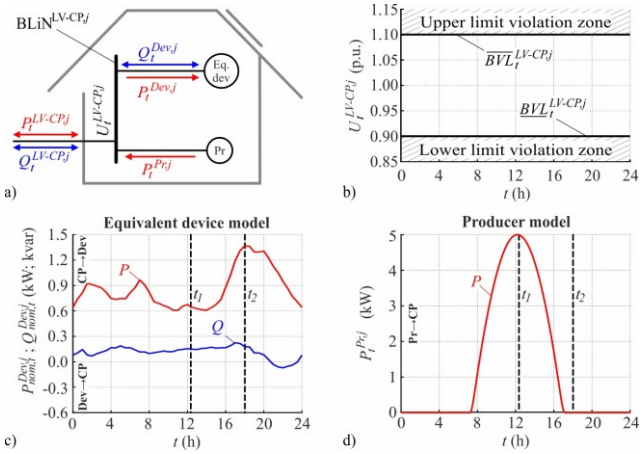

Fig. 5 Lumped model of residential CP_Link-Grids: (a) structure; (b) BVLs; (c) load profiles of the equivalent device model; (d) load profile of the producer model.

The active ($P_t^{Dev,j}$) and reactive power ($Q_t^{Dev,j}$) contributions of the equivalent device model vary over time and voltage ($U_t^{LV\text{-}CP_j}$) at the BLiN$^{\text{LV-CP}_j}$. They are defined by the load profiles shown in Fig. 5c for nominal voltage (U_{nom}). The capacitive behaviour in the evening results from the use of light-emitting diodes (LED) and other modern appliances [5]. Voltage dependency is reflected by Eq. (1) wherein time-variant ZIP-coefficients from [6] are used.

$$\frac{P_t^{Dev,j}}{P_{nom,t}^{Dev,j}} = C_t^{Z,P} \cdot \left(\frac{U_t^{LV\text{-}CP_j}}{U_{nom}}\right)^2 + C_t^{I,P} \cdot \left(\frac{U_t^{LV\text{-}CP_j}}{U_{nom}}\right) + C_t^{P,P} \quad (1a)$$

$$\frac{Q_t^{Dev,j}}{Q_{nom,t}^{Dev,j}} = C_t^{Z,Q} \cdot \left(\frac{U_t^{LV\text{-}CP_j}}{U_{nom}}\right)^2 + C_t^{I,Q} \cdot \left(\frac{U_t^{LV\text{-}CP_j}}{U_{nom}}\right) + C_t^{P,Q} \quad (1b)$$

$$C_t^{Z,P} + C_t^{I,P} + C_t^{P,P} = C_t^{Z,Q} + C_t^{I,Q} + C_t^{P,Q} = 1 \quad (1c)$$

Where $C_t^{Z,P}$, $C_t^{I,P}$, $C_t^{P,P}$ and $C_t^{Z,Q}$, $C_t^{I,Q}$, $C_t^{P,Q}$ are the *P*- and *Q*-related ZIP-coefficients; and $P_{nom,t}^{Dev,j}$, $Q_{nom,t}^{Dev,j}$ are the power contributions of the equivalent device model for nominal voltage. The active power injection of the producer model ($P_t^{Pr,j}$) is determined by the load profile shown in Fig. 5d and does not depend on the voltage. The instants of time with maximal active power absorption and injection are marked in Fig. 5c-d and denoted as t_1 and t_2, respectively.

3.2.2 Low voltage grid

The theoretical LV grid shown in Fig. 6a is analysed in detail to illustrate the concept of BVLs. It includes a distribution transformer (DTR) with a rating of 160 kVA and one feeder with the length *l* that equidistantly connects *N* residential CP_Link-Grids. Two different conductor types are considered separately: overhead line and cable; their parameters are given in Table 1.

Table 1 Parameters of cable and overhead line conductors

Conductor	R' (Ohm/km)	X' (Ohm/km)	C' (nF/km)
Cable	0.2060	0.0800	1040
Overhead line	0.3264	0.3557	0

Fig. 6b shows the lumped LV_Link-Grid model that is intended to be used for load flow analysis in MV level. The corresponding BVLs are calculated and discussed in section 4.

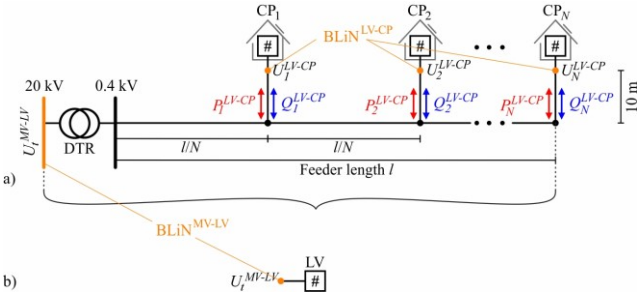

Fig. 6 Model of the LV level: (a) detailed; (b) lumped.

4 Variable boundary voltage limits

The boundary voltage limits of the lumped LV_Link-Grid model are calculated by a series of load flow simulations within the detailed LV_Link-Grid model.

4.1 The rise of variable boundary voltage limits

The voltage profiles of the cable feeder (l = 1 km, N = 25) at t_1 and t_2 are shown in Fig. 7 for MV-LV boundary voltages that provoke violations of the upper and lower LV-CP boundary voltage limits. At 12:10, the upper $BVL^{LV\text{-}CP}$ is violated by the backmost CP (j = 25) when the MV-LV boundary voltage exceeds 1.031 p.u., setting the upper $BVL^{MV\text{-}LV}$ accordingly, Fig. 7a and Eq. (2a). When the MV-LV boundary voltage is reduced to 0.889 p.u., the lower $BVL^{LV\text{-}CP}$ is violated by the foremost CP (j = 1), Fig. 7b and Eq. (2b). In this case, the lower limit is less restrictive at the BLiN$^{\text{MV-LV}}$ than at the BLiN$^{\text{LV-CP}}$.

$$\overline{BVL}_{12:10}^{MV\text{-}LV} = \overline{BVL}_{12:10}^{LV\text{-}CP,25} - |\Delta U_{12:10}^{upper}| = 1.031 \text{ p.u.} \quad (2a)$$

$$\underline{BVL}_{12:10}^{MV\text{-}LV} = \underline{BVL}_{12:10}^{LV\text{-}CP,1} - |\Delta U_{12:10}^{lower}| = 0.889 \text{ p.u.} \quad (2b)$$

Where $\Delta U_{12:10}^{upper}$, $\Delta U_{12:10}^{lower}$ are the voltage drops between the BLiN$^{\text{MV-LV}}$ and the upper and lower limit violating BLiN$^{\text{LV-CP}}$, respectively, at 12:10. At 18:00, the voltages decrease along the DTR and LV feeder, setting the upper and lower MV-LV boundary voltage limits to 1.105 and 0.927 p.u., respectively, Fig. 7c-d and Eq. (3).

$$\overline{BVL}_{18:00}^{MV\text{-}LV} = \overline{BVL}_{18:00}^{LV\text{-}CP,1} - |\Delta U_{18:00}^{upper}| = 1.105 \text{ p.u.} \quad (3a)$$

$$\underline{BVL}_{18:00}^{MV\text{-}LV} = \underline{BVL}_{18:00}^{LV\text{-}CP,25} - |\Delta U_{18:00}^{lower}| = 0.927 \text{ p.u.} \quad (3b)$$

Where $\Delta U_{18:00}^{upper}$, $\Delta U_{18:00}^{lower}$ are the voltage drops between the $BLiN^{MV\text{-}LV}$ and the upper and lower limit violating $BLiN^{LV\text{-}CP}$, respectively, at 18:00.

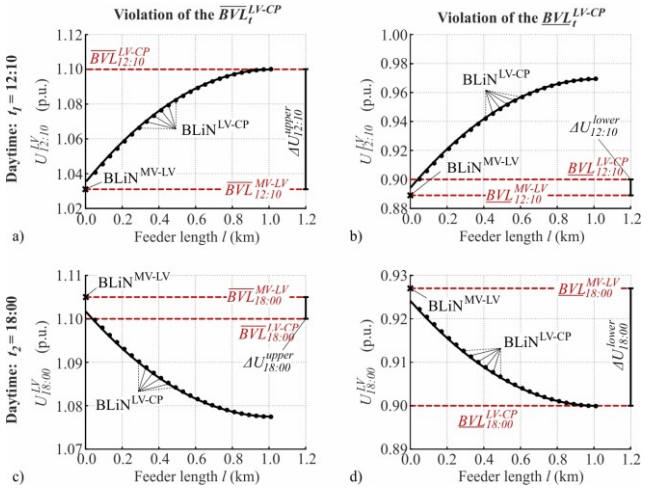

Fig. 7 Voltage profiles of the cable feeder (l = 1 km, N = 25) for MV-LV boundary voltages that provoke violations of the LV-CP boundary voltage limits: a) upper limit at t_1; b) lower limit at t_1; c) upper limit at t_2; b) lower limit at t_2.

The calculation of the load flows for the entire time horizon results in the variable BVLs of the lumped LV_Link-Grid model. They are shown – together with the (constant) LV-CP boundary voltage limits – in Fig. 8.

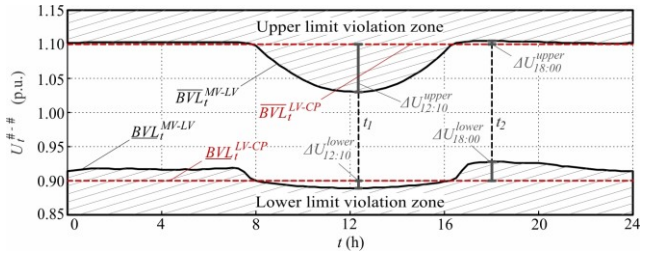

Fig. 8 Deformation of the boundary voltage limits by the internal voltage drops of the LV_Link-Grid (cable, l = 1 km, N = 25).

The voltage drops in the LV_Link-Grid deform the boundary voltage limits seen from the MV_Link-Grid. The injection of the PV systems around noontime decreases both, the lower and especially the upper $BVL^{MV\text{-}LV}$. Meanwhile, the power absorption in the evening increases both $BVL^{MV\text{-}LV}$, narrowing the permissible voltage range in total.

4.2 Effects of feeder properties

The degree of the BVL deformation depends on the feeder properties, i.e. the conductor type, the feeder length, and the number of connected CPs, Fig. 7. A clear trend is observed for all properties. In all cases, the overhead line conductor provokes greater deformations than the cable one. An increasing number of connected CPs intensifies the deformation. Furthermore, long feeders deform the voltage limits more than short feeders.

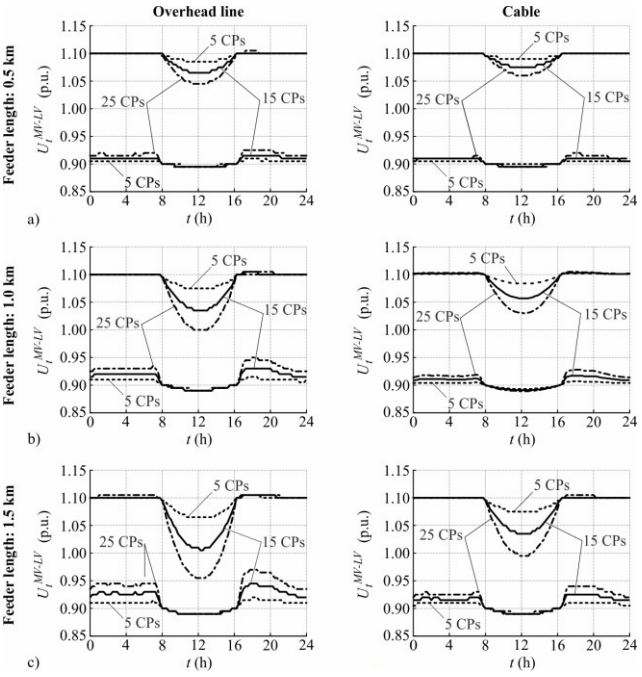

Fig. 9 MV-LV boundary voltage limits for overhead line and cable conductor, 5, 15, and 25 connected CPs and different feeder lengths: (a) 0.5 km; (b) 1.0 km; (c) 1.5 km.

4.3 Discussion

The BVL deformation between $BLiN^{MV\text{-}LV}$ and $BLiN^{LV\text{-}CP}$ results from the internal voltage drops of the LV_Link-Grid. This voltage drop depends on the power flows through the grid, the series impedances of the grid, and the MV-LV boundary voltage. These basic considerations allow to understand the observed effects of the distinct feeder properties. The overhead line conductor has greater series resistance and reactance than the cable one, thus causing higher voltage drops along the feeder. The series impedance increases – for both conductor types – linearly with the feeder length, leading to greater voltage drops over longer feeders. An increase in the CP number increases the power flows through the grid, because they all contribute power simultaneously. This intensifies the voltage drop over the feeder.

5 Use case: notification of boundary voltage limits

The introduced concept enables smart grids to be operated closer to their factual limits. By applying the *LINK*-based holistic architecture, a use case is formulated that applies in different timeframes, e.g. in day ahead and in real-time.

5.1 General description

Fig. 10 gives an overview of the use case 'Notification of $BVL^{MV\text{-}LV}$'. It may be used in two distinct cases:

- **Different operators operate MV_ and LV_Grid-Links.** This case is shown in Fig. 10, where the medium (MVSO) and low voltage system operators (LVSO) operate the Grid-Links, which may be different companies. The LVSO calculates the MV-LV boundary voltage limits and notifies them to the MVSO. The MVSO receives individual $BVL^{MV\text{-}LV}$ from each connected LV_Grid-Link and sets the optimization constraints of its Volt/var secondary control (Vv**SC**^{MV}) accordingly.

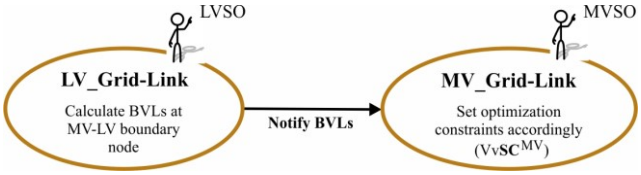

Fig. 10 Overview of the use case: notification of $BVL^{MV\text{-}LV}$: Different operators operate the MV_ and LV_Grid-Links.

- **The same operator operates MV_ and LV_Grid-Links.** This is the common case today where the DSO operates both, the MV and LV grids, Fig. 11. Although the data for the grids of both voltage levels are normally available in the same database, the state estimation may be performed from different applications and in different time intervals. In this case, the $BVL^{MV\text{-}LV}$ can be calculated separately and off-line, and can be provided for the online calculations of the MV grids.

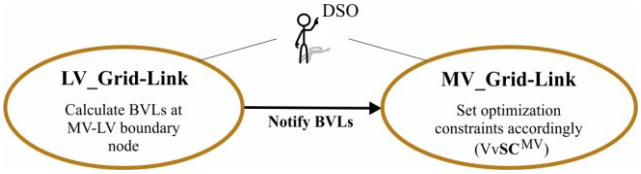

Fig. 11 Overview of the use case: notification of $BVL^{MV\text{-}LV}$: The same operator operates the MV_ and LV_Grid-Links.

5.2 Day ahead scheduling

The LVSO calculates the day-ahead schedule of the MV-LV boundary voltage limits with sufficient resolution and notifies it to the MVSO. The MVSO receives individual day-ahead schedules from each connected LV_Grid-Link and sets the (time-variant) optimization constraints of its Vv**SC**^{MV} for the next day accordingly.

5.3 Short term adaptation

The LVSO recognizes a deviation from its actual day-ahead schedule of the MV-LV boundary voltage limits, recalculates the $BVL^{MV\text{-}LV}$ and notifies them to the MVSO. The MVSO receives adapted MV-LV boundary voltage limits from various LV_Grid-Links and updates the optimization constraints of its Vv**SC**^{MV} accordingly.

6 Conclusion

The use of time constant voltage limits to check the power flow results is not accurate. Voltage limits in radial structures (e.g. MV) are object to deformation due to the voltage drops in the subordinated grids (e.g. LV). The extent of this deformation depends on the properties of the LV feeders: the greater the feeder impedance and the number of connected customer plants, the more intensive is the deformation. In order to take the latter into account, the lumped grid models are extended with a new parameter "The boundary voltage limit". It allows to verify the voltage limit compliance in low voltage level by conducting load flow analysis in medium voltage level. This concept may be used to increase the operational efficiency of smart grids by day ahead scheduling and short-term (online) adaption of the MV-LV boundary voltage limits.

6 References

[1] EN 50160: 'Voltage characteristics of electricity supplied by public electricity networks', 2010.

[2] Bletterie, A., et al.: 'Enhancement of the network hosting capacity – clearing space for/with PV'. Proc. 25th European Photovoltaic Solar Energy Conference and Exhibition, Valencia, Spain, Sept. 2010, pp. 4828–4834.

[3] Ilo, A.: '"Link" – The smart grid paradigm for a secure decentralized operation architecture', Electr. Power Syst. Res., 2016, 131, pp. 116–125.

[4] Ilo, A.: 'Design of the Smart Grid Architecture According to Fractal Principles and the Basics of Corresponding Market Structure', Energies, 2019, 12, 4153.

[5] Schultis, D.-L., Ilo, A.: 'Adaption of the Current Load Model to Consider Residential Customers Having Turned to LED Lighting'. Proc. 2019 IEEE PES Asia-Pacific Power and Energy Engineering Conference (APPEEC), Macao, Macao, Dec. 2019, pp. 1–5.

[6] Schultis, D.-L.: 'Daily load profiles and ZIP models of current and new residential customers', Mendeley Data, V1, 2019. (dataset)